

NEURITE ORIENTATION DISPERSION AND DENSITY IMAGING OF THE CERVICAL CORD IN VIVO

Francesco Grussu¹, Torben Schneider¹, Hui Zhang², Daniel C. Alexander², and Claudia A. M. Wheeler-Kingshott¹

¹NMR Research Unit, Department of Neuroinflammation, Queen Square MS Centre, UCL Institute of Neurology, London, England, United Kingdom, ²Department of Computer Science and Centre for Medical Image Computing, University College London, London, England, United Kingdom

TARGET AUDIENCE Scientists with interest in diffusion MRI of the spinal cord *in vivo*.

PURPOSE To demonstrate Neurite Orientation Dispersion and Density Imaging (NODDI)¹ in the healthy cervical cord *in vivo*.

INTRODUCTION Advanced diffusion MRI techniques can provide more specific information than standard Diffusion Tensor Imaging (DTI)², but to date, technical challenges^{3–5} have prevented their routine use in the spinal cord *in vivo*. For this purpose, NODDI is promising as it can probe specific microstructural features in a clinically feasible time¹. Such features relate to neurite architecture and are potential markers for neurodegenerative diseases, such as multiple sclerosis, which can have devastating effects on the spinal cord⁶. Here, we analyse multi-shell diffusion data of the cervical cord *in vivo* with NODDI for the first time, assess the reproducibility of its metrics and their relation to DTI indices.

METHODS Data We scanned 5 healthy volunteers (subjects S1 to S5, 2 males, mean age 36 years, range 25–47) on a 3T Philips Achieva scanner at cervical level (C1 to C5). Subjects S1 to S3 were recalled for a second scan. We followed the NODDI protocol¹ (30 directions at $b = 711 \text{ s mm}^{-2}$ and 60 at $b = 2855 \text{ s mm}^{-2}$), acquiring 12 axial slices with a cardiac-gated PGSE ZOOM-EPI sequence (TE = 65.5 ms, $\Delta = 32.2$ ms, $\delta = 20.5$ ms, TR = 12 RRs, reduced FOV of $64 \times 48 \text{ mm}^2$, SENSE factor of 1.5, resolution of $1 \times 1 \times 5 \text{ mm}^3$, scan time of approximately 35 minutes).

Preprocessing We corrected for motion slice-by-slice with FSL FLIRT⁷ and drew a cord mask⁸ (*fitting mask*) on the mean $b = 0$ slices which was cropped to the 6 central slices (*analysis mask*) to provide anatomical correspondence across subjects and scans.

Fitting NODDI and DTI models were fitted within the *fitting mask* of all scans with the NODDI MATLAB toolbox and Camino⁹ respectively. We used both b shells for NODDI and the $b = 711 \text{ s mm}^{-2}$ shell only for DTI, to limit the contribution of non-Gaussian diffusion³. Analysis focused on the following metrics. For NODDI: the isotropic volume fraction (v_{iso}); the intra-neurite volume fraction (v_{in}), such that the volume fraction of the voxel occupied by neurites is $v_r = (1 - v_{\text{iso}}) v_{\text{in}}$; the orientation dispersion index (ODI). For DTI: fractional anisotropy (FA), axial, radial and mean diffusivities (AD, RD and MD respectively).

Reproducibility Scan–rescan reproducibility of both DTI and NODDI was assessed with S1, S2 and S3 by comparing the mean values of each metric within the *analysis mask* of the two scans with a coefficient of variation (CV). For each metric and each subject, we calculated the CV as $CV = 100 \sigma / m$, with m and σ indicating quantities $m = (\frac{1}{2} m_1 + \frac{1}{2} m_2)$ and $\sigma = (\sqrt{(m_1 - m)^2 + (m_2 - m)^2})^{1/2}$. Here, m_i stands for the mean value of the studied metric within the *analysis mask* of scan $i = 1, 2$.

Relationship with DTI We investigated the relationship between DTI and NODDI indices *in vivo* by colour-coding scatter plots (v_{in} , ODI) according to FA, AD, RD and MD. We omitted rescans, focusing on *analysis mask* voxels where i) $v_{\text{iso}} \leq 0.05$, to discard areas with CSF contamination, and ii) the considered DTI metric ranged between the 5th and the 95th percentile of its distribution across the 5 data sets, to remove outliers. For comparison, we evaluated the patterns of DTI indices which would be observed in a tissue perfectly matching NODDI model assumptions as follows. We synthesized the NODDI diffusion-weighted signal produced by the $b = 711 \text{ s mm}^{-2}$ shell for $\text{SNR} \rightarrow \infty$ and for $v_{\text{iso}} = 0$, varying v_{in} and ODI in a grid of 64×64 uniform values in $[0.05; 0.95] \times [0.005; 0.5]$ and fixing the mean orientation and the intrinsic free diffusivity¹ to $\mu = [0 \ 0 \ 1]^T$ and $d_{\parallel} = 1.7 \text{ } \mu\text{m}^2 \text{ ms}^{-1}$. Then, we added Rician noise to the measurements ($\text{SNR} := S(0) / \sigma_{\text{noise}}$ of 10) and fitted the DTI model with Camino to visualize DTI metrics as functions of v_{in} and ODI.

RESULTS Metrics Figure 1 shows that v_{iso} was high at the cord border and in an area corresponding with the location of the anterior median fissure, where CSF partial volume is likely. In all those voxels, v_{in} was also high but the total volume fraction v_r was low. Lastly, ODI appeared higher in gray matter compared to white matter.

Reproducibility The average CV over S1, S2, S3 was 4.19 % for v_{iso} ; 2.50 % for v_{in} ; 6.88 % for ODI; 2.02 % for FA; 3.23 % for AD; 1.10 % for RD; 2.35 % for MD.

Relationship with DTI Figure 2 shows that very different combinations of v_{in} and ODI can theoretically produce similar values of DTI indices for $\text{SNR} \rightarrow \infty$ and even for $\text{SNR} = 10$. Scatter plots from *in vivo* data well-replicated theoretical patterns in the observed range, confirming trends seen in the brain¹. As an example, our analysis suggested that a decrease in FA may be caused independently by either increasing neurite orientation dispersion or decreasing neurite density.

DISCUSSION AND CONCLUSION This is the first demonstration of NODDI with multi-shell diffusion MRI data in the spinal cord *in vivo*. Firstly, several known anatomical features could be identified in NODDI metrics, replicating findings in the brain¹. Secondly, the reproducibility of the technique was comparable to that of routine DTI, although the DTI model was fitted to a fewer measurements than NODDI and its reproducibility may be affected. Thirdly, the relationships between NODDI and DTI parameters seen in the brain¹ were confirmed, with the former giving a more intuitive description of the microstructure of the spinal cord compared to the latter. Therefore, NODDI can be a feasible and more specific alternative to DTI for *in vivo* diffusion MRI of the spinal cord, potentially able to disentangle tissue damage mechanisms involving neurite orientation dispersion and density separately. As future work, we will optimize the acquisition for cord anatomy to reduce the scan time and further validate the specificity of NODDI parameters with histological analysis.

ACKNOWLEDGEMENTS The MS Society in UK, NIHR UCL–UCLH BRC, UCL GCS, all volunteers.

REFERENCES 1. Zhang H et al. NeuroImage (NI) (2012); 61(4): 1000–16. 2. Basser PJ et al. Biophys J (1994); 66(1): 259–67. 3. Farrell JAD et al. MRM (2008); 59(5): 1079–89. 4. Mohammadi S et al. NI (2013); 70: 377–85. 5. Rangwala NA et al. NI (2013); 82: 416–25. 6. Lukas C et al. Radiology (2013); 269(2): 542–52. 7. Jenkinson M et al. NI (2002); 17(2): 825–41. 8. Horsfield MA et al. NI (2010); 50(2): 446–55. 9. Cook PA et al. Proc ISMRM (2006); p.2759.

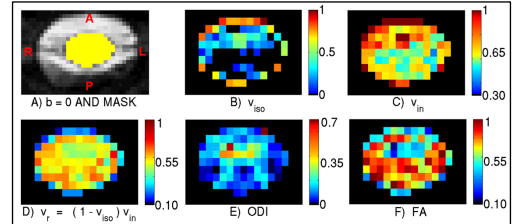


Figure 1: *fitting mask*, mean $b = 0$ (in A) and metrics (from B to F) in 10th slice of S1, first scan.

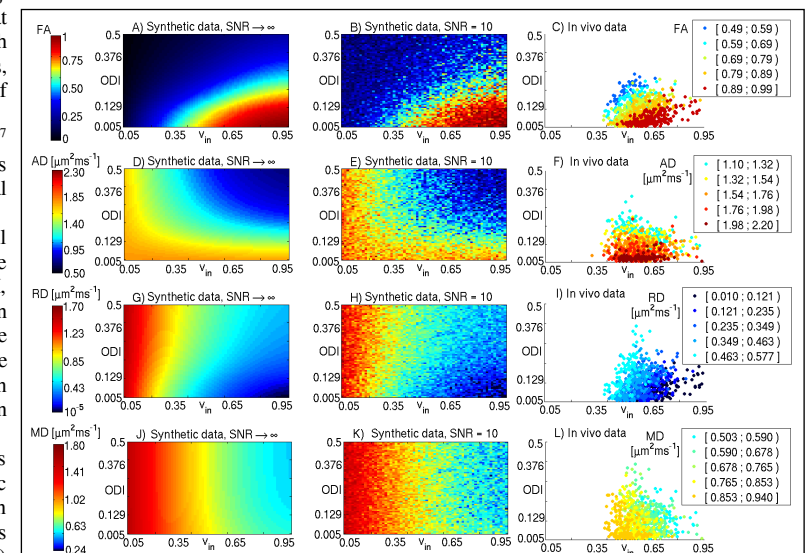


Figure 2: theoretical relationships between DTI and NODDI metrics for $\text{SNR} \rightarrow \infty$ (left column) and for $\text{SNR} = 10$ (central column). Corresponding scatter plots (v_{in} , ODI) from *in vivo* data colour-coded by DTI indices (right column).